Internal Medicine
The Japanese Society of Internal Medicine
doi: 10.2169/internalmedicine.2742-23
Intern Med 63: 1575-1584, 2024
http://internmed.jp

【 CASE REPORT 】

A Gluteus Medius Muscle Biopsy to Confirm Amyloid Transthyretin Deposition in Wild-type Transthyretin Cardiac Amyloidosis: A Report of Two Cases

Koji Takahashi[1,2], Takaaki Iwamura[3], Yoshiyasu Hiratsuka[3], Daisuke Sasaki[3], Nobuhisa Yamamura[4], Mitsuharu Ueda[5], Hiroe Morioka[2], Mako Yoshino[2], Daijiro Enomoto[2], Shigeki Uemura[2], Takafumi Okura[2], Tomoki Sakaue[1,2] and Shuntaro Ikeda[1,2]

Abstract:
In patients with wild-type transthyretin cardiac amyloidosis (ATTRwt-CA), the uptake of the tracer on technetium-99m-labeled pyrophosphate (^{99m}Tc-PYP) scintigraphy, which indicates amyloid transthyretin (ATTR) *per se*, is often observed in skeletal muscles, such as the abdominal oblique and gluteal muscles. Among extracardiac biopsies for confirming ATTR deposition in ATTRwt-CA, a ^{99m}Tc-PYP imaging-based computed tomography (CT)-guided core needle biopsy of the internal oblique muscle has relatively high sensitivity. In some patients, the ^{99m}Tc-PYP uptake is more pronounced in the gluteal muscles than in oblique muscles. We herein report two cases of ATTRwt-CA in which a CT-guided biopsy of the gluteus medius muscle with ^{99m}Tc-PYP uptake confirmed the presence of ATTR deposits.

Key words: bone-avid tracer, case report, computed tomography, core needle biopsy, gluteus medius muscle, wild-type transthyretin amyloidosis

(Intern Med 63: 1575-1584, 2024)
(DOI: 10.2169/internalmedicine.2742-23)

Introduction

We previously reported that the tracer uptake in technetium-99m-labeled pyrophosphate (^{99m}Tc-PYP) scintigraphy can be detected in some skeletal trunk muscles of patients with wild-type transthyretin (ATTRwt) cardiac amyloidosis (CA), although findings differ among patients and their skeletal muscles (1). In addition, based on the concept that ^{99m}Tc-PYP scintigraphy can image the extracardiac tracer uptake, demonstrating the amyloid transthyretin (ATTR) burden (2-4), we subsequently reported the feasibility of using a ^{99m}Tc-PYP imaging-based computed tomography (CT)-guided core needle biopsy of the internal oblique muscle, which has the highest uptake rate among the 11 skeletal trunk muscles studied (1), as an extracardiac screening biopsy to confirm the presence of ATTR deposition in ATTRwt-CA cases (5).

Among the 11 skeletal trunk muscles, the gluteal muscles have the second-highest ^{99m}Tc-PYP uptake rate, after the oblique muscles (1). In some patients, however, the ^{99m}Tc-PYP uptake is more pronounced in the gluteal muscles than in the oblique muscles.

We herein report two ATTRwt-CA cases in which a ^{99m}Tc-PYP imaging-based CT-guided core needle biopsy of the gluteus medius muscle confirmed ATTR deposition.

Case Reports

Case 1

A 94-year-old Japanese woman was transferred from an-

[1]Department of Community Emergency Medicine, Ehime University Graduate School of Medicine, Japan, [2]Department of Cardiology, Yawatahama City General Hospital, Japan, [3]Department of Radiology, Yawatahama City General Hospital, Japan, [4]Department of Clinical Pathology, Yawatahama City General Hospital, Japan and [5]Department of Neurology, Graduate School of Medical Sciences, Kumamoto University, Japan
Received: August 9, 2023; Accepted: September 14, 2023; Advance Publication by J-STAGE: October 27, 2023
Correspondence to Dr. Koji Takahashi, michitokitatsumasa@gmail.com

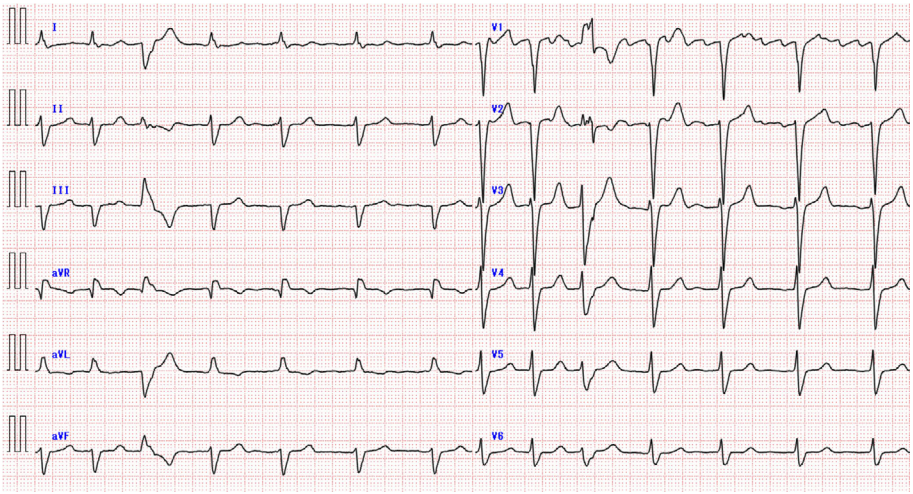

Figure 1. Electrocardiogram findings recorded on admission (Case 1). Atrial flutter with flutter waves at a rate of 271/min (cycle length, 221 ms) and irregular ventricular rate, left axis deviation, poor R-wave progression, nonspecific intraventricular conduction delay with a QRS complex duration of 144 ms, and premature ventricular contraction are shown.

other clinic to Yawatahama City General Hospital with a fever of unknown origin. The patient had previously undergone surgery for a thyroid tumor and been prescribed levothyroxine sodium hydrate (50 μg once daily) for hypothyroidism after thyroidectomy at the same clinic. One month prior to presentation at our hospital, the patient was admitted to the clinic for left upper extremity paralysis due to right frontal lobe infarction caused by a cardiac embolus. In addition, the patient was being administered rivaroxaban (10 mg once daily) for atrial fibrillation. The patient had no history of orthopedic diseases considered to be extracardiac manifestations of ATTRwt amyloidosis, such as carpal tunnel syndrome or spinal canal stenosis. Furthermore, the patient did not complain of muscle weakness or cramps, which would raise the suspicion of amyloid myopathy (6).

The patient's vital signs were as follows: temperature, 36.5°C; pulse rate, 67 beats/min; systemic blood pressure, 112/88 mmHg; and oxygen saturation (measured on room air using a pulse oximeter), 97%. Physical examination findings were unremarkable, except for left hemiparesis with manual muscle testing 3/5 in the left upper and lower extremities, irregular heartbeat, and swelling and redness in the right-hand joint. Blood tests revealed an elevated C-reactive protein level of 1.25 mg/dL (reference range, ≤0.7 mg/dL) and brain natriuretic peptide level of 210.9 pg/mL (reference range, ≤18.4 pg/mL). The patient's creatine kinase level (29 U/L) was normal (reference range, ≤165 U/L). Electrocardiography revealed atrial flutter (Fig. 1). Echocardiography revealed left atrial dilation and a reduced left ventricular (LV) systolic function with increased wall thickening and apical sparing (Fig. 2). CT revealed no potential sources of the fever but did show hemorrhagic transformation of the cerebral infarct.

The patient was diagnosed with right wrist arthritis and prescribed a nonsteroidal anti-inflammatory drug. Rivaroxaban was discontinued because of hemorrhagic infarction. Based on the electrocardiography and echocardiography findings, CA was suspected. Monoclonal protein studies on immunofixation electrophoresis of both serum and urine and serum-free light chain assays did not show monoclonal gammopathy. ^{99m}Tc-PYP scintigraphy was performed two hours after tracer injection, as previously reported (1-5) and according to the American Society of Nuclear Cardiology consensus recommendations (7). Perugini grade 3 myocardial uptake with a heart-to-contralateral lung ratio of 1.97 was revealed. In addition, myocardial and extracardiac uptakes were confirmed using single-photon emission CT (SPECT)/CT fusion images (Fig. 3). Regarding the extracardiac accumulation of ^{99m}Tc-PYP, the tracer uptake in the gluteal muscles, including the minimus, medius, and maximus muscles, was more pronounced than its uptake in the abdominal oblique muscles. The tracer uptake in the subcutaneous abdominal fat with a mottled uptake pattern was also detected.

First, the patient underwent a subcutaneous abdominal fat fine-needle aspiration biopsy three days after ^{99m}Tc-PYP scintigraphy. Because amyloid deposition was minimal in the specimens obtained, amyloid typing by immunohistochemical staining was deemed unlikely to be successful. Thus, the patient underwent a ^{99m}Tc-PYP imaging-based CT-guided core needle biopsy of the gluteus medius muscle, as described in a previous study (5), nine days after ^{99m}Tc-PYP scintigraphy (Fig. 4). Six punctures were made, and 4 cores ≥1 mm^3 in size were obtained. Therefore, the amount of muscle tissue obtained was considered to be sufficient. The duration of the procedure was 40 min. The dose-length product and effective dose were 884.3 mGy·cm and 17.7 mSv, respectively. Complications, such as local pain and hematoma, have not been reported. The presence of amyloid deposition in the tissue samples was detected using Congo red staining performed at Kumamoto University, and an im-

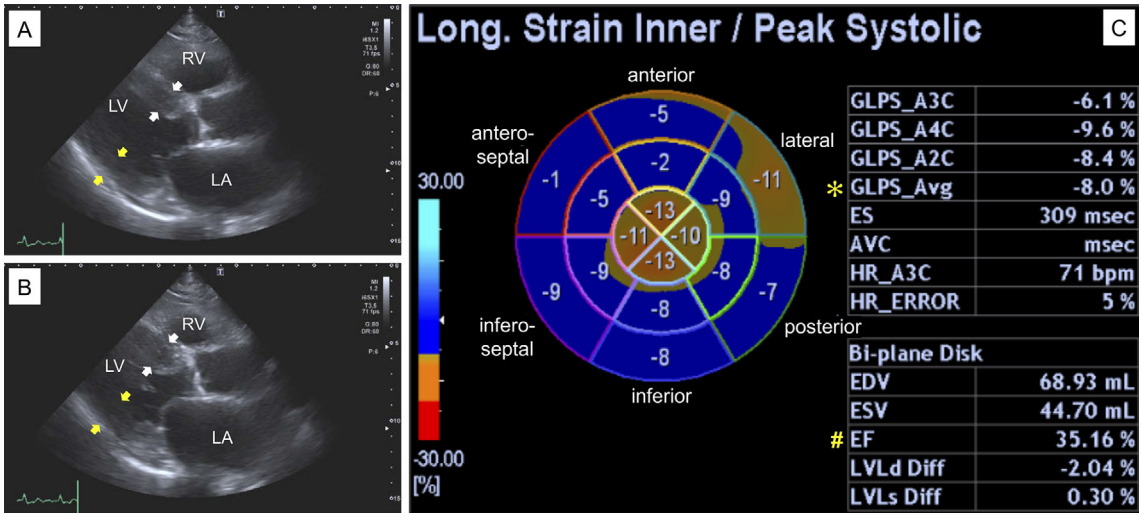

Figure 2. Transthoracic echocardiogram findings recorded on admission (Case 1). A normal-sized left ventricle with an end-diastolic dimension of 43.1 mm and an increase in the interventricular septum (white arrows) and left ventricular (LV) posterior wall (yellow arrows) of 14.6 and 14.8 mm, respectively, are shown (A, end-diastole; B, end-systole). The bull's-eye map (with the apex at the center of the color-coding map) illustrates segmental longitudinal LV peak systolic strain values of the 16-segment model generated by the speckle-tracking analysis of 2-dimensional LV images acquired from apical 2-, 3-, and 4-chamber views (A2C, A3C, and A4C, respectively). A reduced LV ejection fraction (EF) of 35.2% (marked with a hash mark) is shown as well as an LV global longitudinal peak systolic strain (GLS) value of -8.0% (calculated as the mean of these 16 values; marked with an asterisk) with an LVEF/|GLS| of 4.4, indicating apical sparing (cutoff, >4.1) (C). The left atrium, with a volume of 62.5 mL/m^2, was dilated (A, B). LA: left atrium, LV: left ventricle, RV: right ventricle

munohistochemical analysis performed at the same institution confirmed ATTR deposition (Fig. 5). Transthyretin (TTR) gene sequencing did not reveal any genetic variants. Therefore, the patient was diagnosed with ATTRwt-CA. However, the patient was not prescribed tafamidis because of frailty.

Case 2

An 86-year-old Japanese man with heart failure was admitted to Yawatahama City General Hospital. The patient had previously undergone surgery for kidney stones, benign prostatic hypertrophy, and stomach cancer and had been prescribed amlodipine besilate (2.5 mg once daily), edoxaban tosilate hydrate (30 mg once daily), verapamil hydrochloride (40 mg thrice daily), bisoprolol (4 mg once daily), and spironolactone (12.5 mg once daily) for long-standing hypertension and a 3-year history of paroxysmal atrial fibrillation/flutter at another clinic. The patient did not have a history of orthopedic diseases considered to be extracardiac manifestations of ATTRwt amyloidosis, such as carpal tunnel syndrome or spinal canal stenosis. In addition, the patient did not complain of muscle weakness or cramps that might indicate amyloid myopathy (6).

The patient's vital signs were as follows: temperature, 36.4°C; pulse rate, 111 beats/min; systemic blood pressure, 114/74 mmHg; and oxygen saturation (measured on room air using a pulse oximeter), 98%. Physical examination findings were unremarkable except for irregular heartbeats and mild pretibial edema. Blood tests revealed an elevated brain natriuretic peptide level (173.2 pg/mL; reference range, ≤ 18.4 pg/mL), but the high-sensitivity cardiac troponin I level (12.5 pg/mL; reference range, ≤18.4 pg/mL) and creatine kinase concentration (57 U/L; reference range, ≤190 U/L) were normal. Chest radiography revealed mild pulmonary congestion. Electrocardiography revealed atrial tachycardia (Fig. 6). Echocardiography demonstrated left atrial dilation and a reduced LV systolic function, with increased wall thickening and apical sparing (Fig. 7).

The patient was suspected of having CA. Monoclonal protein studies using immunofixation electrophoresis of serum, immunofixation electrophoresis of urine, and serum-free light-chain assays did not detect plasma cell dyscrasia. ^{99m}Tc-PYP scintigraphy, performed using the same acquisition parameters as those reported in Case 1, revealed a Perugini grade 2 myocardial uptake with a heart-to-contralateral lung ratio of 1.26, which was confirmed using SPECT/CT fusion images (Fig. 8). The ^{99m}Tc-PYP tracer uptake in the gluteus, particularly in the minimus and medius muscles, was more pronounced than in the abdominal oblique muscles. However, no tracer uptake was observed in the subcutaneous abdominal fat.

Twenty-four days after ^{99m}Tc-PYP scintigraphy, the patient underwent a ^{99m}Tc-PYP imaging-based CT-guided core needle biopsy of the gluteus medius muscle, as previously described (5), with administration of edoxaban tosilate hydrate (Fig. 9). Eleven punctures were made, and 7 cores ≥1 mm^3

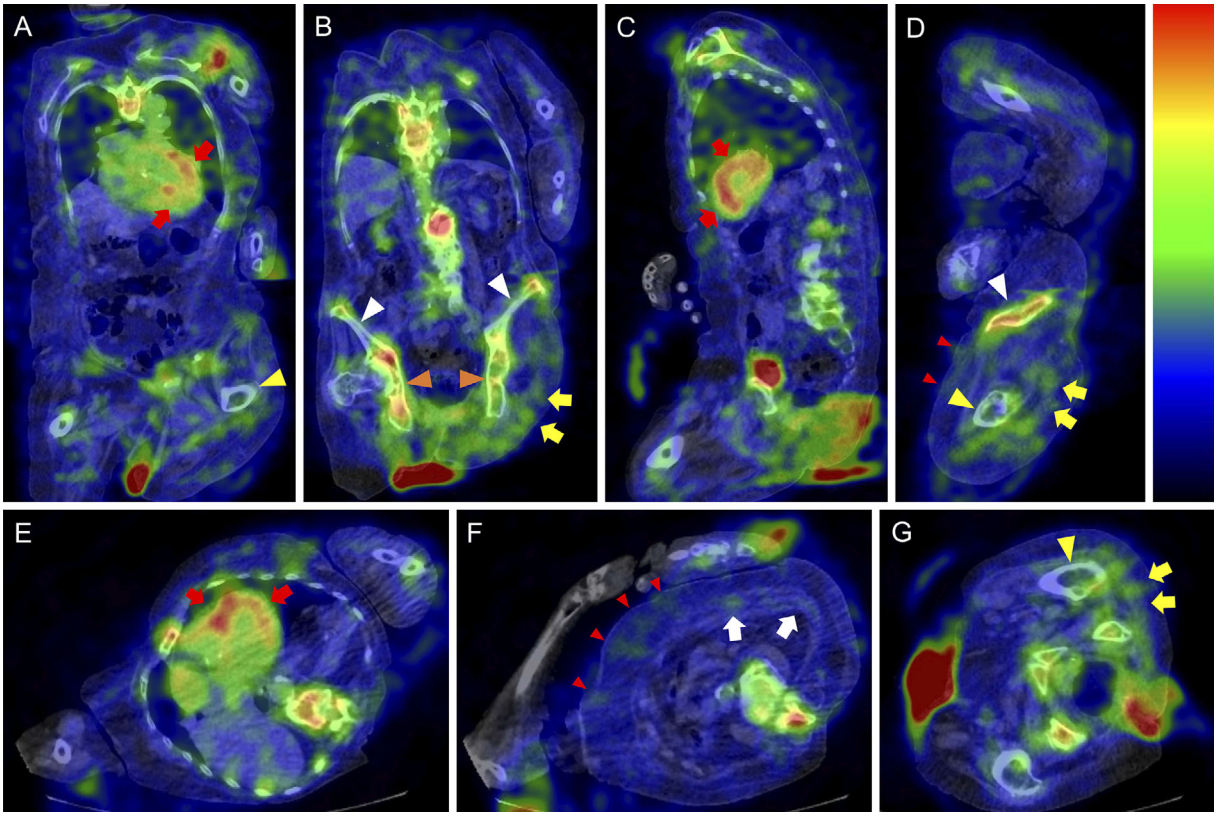

Figure 3. **Chest- and abdomen-centered single-photon emission computed tomography/computed tomography fusion images of technetium-99m-labeled pyrophosphate (^{99m}Tc-PYP) scintigraphy obtained 2 h after injecting the radiotracer (Case 1). (A, B) The coronal plane, (C, D) sagittal plane, and horizontal plane of (E) the heart and (F, G) abdomen/pelvis. The tracer uptake at the sternum was considered the maximum, with that at other sites expressed as relative values; the images are displayed in color. Positive ^{99m}Tc-PYP accumulation was defined as the detection of the tracer uptake in the relevant muscles, regardless of the degree of the uptake (1, 3, 5). The accumulation of ^{99m}Tc-PYP in the myocardium (red arrows), abdominal oblique (white arrows), and gluteus muscles (yellow arrows) is shown. In addition, a subcutaneous abdominal fat tracer uptake displaying a mottled uptake pattern is also shown (red arrowheads). White, orange, and yellow arrowheads indicate the ilium, ischium, and left femur, respectively. For comparison, a representative case of wild-type transthyretin cardiac amyloidosis with almost no tracer uptake in the skeletal trunk muscles is shown (Supplementary material).**

in size were obtained. Therefore, the amount of muscle tissue obtained was considered to be sufficient. The duration of the procedure was 30 min. The dose-length product and effective dose were 119.0 mGy·cm and 2.4 mSv, respectively. Complications, such as local pain and hematoma, have not been reported. Muscle specimens obtained from the biopsy confirmed ATTR deposition via Congo red staining and immunohistochemical staining performed at Kumamoto University (Fig. 10). The patient was diagnosed with ATTRwt-CA based on the TTR gene sequencing results and started taking tafamidis. For atrial tachycardia, amiodarone hydrochloride was initiated after verapamil hydrochloride was discontinued, resulting in a conversion to sinus rhythm.

Discussion

In this study, a CT-guided core needle biopsy of the gluteus medius muscle with a ^{99m}Tc-PYP uptake, which was performed in two patients with suspected ATTRwt-CA, confirmed ATTR deposition in the muscle specimens obtained.

ATTRwt-CA is a systemic disease characterized by ATTR deposits in most organs, including those that do not show signs of disease. However, the main target organs are the heart, lungs, ligaments, and tenosynovium (8). Immunohistochemical studies have indicated that amyloid deposition varies between organs (9). In addition, we previously reported that the tracer uptake on ^{99m}Tc-PYP scintigraphy differs among patients with ATTRwt-CA and their skeletal muscles (1). However, the reason for this heterogeneity remains unclear. Wild-type ATTR deposits tend to develop in tissues and organs with long-term mechanical stress, such as the heart and spinal ligaments (10-12). This may also be true for skeletal trunk muscles that exhibit high ^{99m}Tc-PYP uptake rates. Among the 11 muscles examined, the abdominal

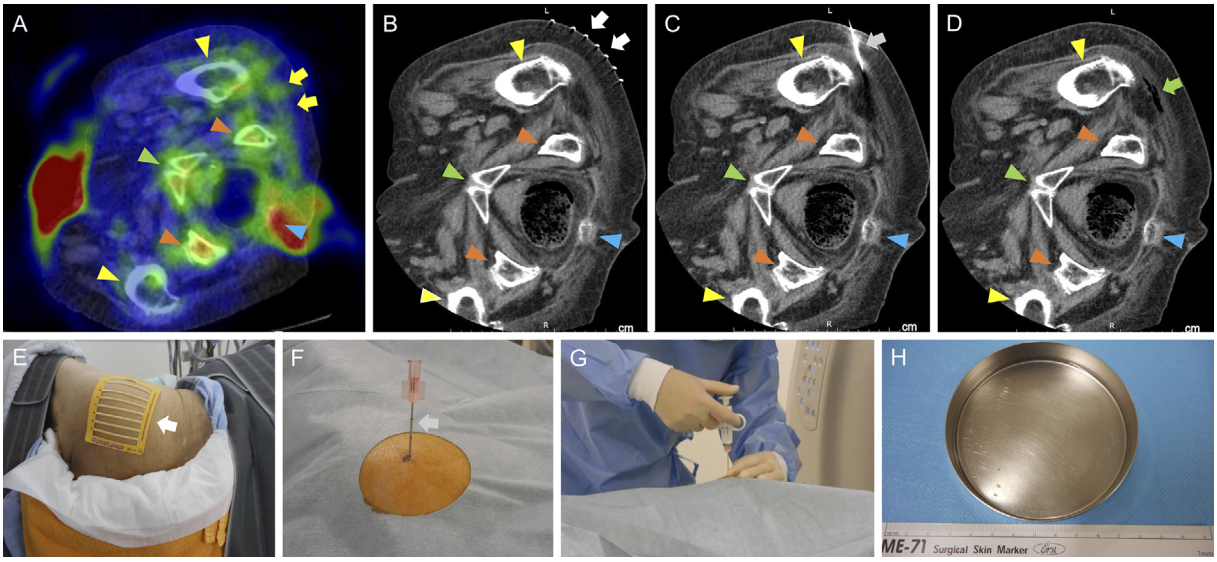

Figure 4. **A technetium-99m-labeled pyrophosphate (^{99m}Tc-PYP) imaging-based computed tomography (CT)-guided core needle biopsy of the left gluteus medius muscle (Case 1). The target of the biopsy was the site with the highest ^{99m}Tc-PYP uptake in the gluteus medius muscle (yellow arrows) (A). The patient was positioned in the supine oblique position on the CT scanner table, and the first CT images were obtained after applying the Guidelines® CT biopsy grid (Beekley Medical, Bristol, USA) to the skin of the biopsy site to optimize the entry site of the biopsy needle and improve the first-stick accuracy (B, E, white arrows). After the biopsy site was cleansed with an iodine solution and the skin, subcutaneous fat tissue, and fascia of the left gluteal muscles were anesthetized with 0.5% procaine hydrochloride, an introducer stylet and cannula (grey arrows) of an 18-gauge Fine Core® (Dr. Japan, Tokyo, Japan) spring-loaded semi-automatic biopsy needle, 10 cm in length, was advanced into the left gluteus medius muscle through a small pre-incision of the skin. After confirming the correct orientation and depth on the CT images acquired, the introducer stylet was retracted (C, F). The biopsy needle was advanced into the introducer cannula left in place (G), and a muscle specimen was obtained (H). No hematoma was observed after retraction of the biopsy needle and introducer cannula, although air was present in the left gluteus medius muscle (light-green arrow) (D). Yellow, light-green, orange, and blue arrowheads indicate the femur, pubis, ischium, and coccyx, respectively.**

oblique muscles showed the highest ^{99m}Tc-PYP uptake rate (94.4%), followed by the gluteal and erector spinae muscles (88.9%) (1).

The diagnosis of amyloidosis is usually based on the presence of amyloid deposits in tissue biopsies (13). An endomyocardial biopsy is the gold standard for diagnosing ATTRwt-CA. Currently, bone-avid radionuclide scintigraphy with comprehensive biochemical tests for monoclonal gammopathy can reliably establish ATTRwt-CA without a biopsy, although approximately 10% of patients with ATTRwt-CA have monoclonal gammopathy and require a biopsy to confirm the presence of ATTR deposition (14). An endomyocardial biopsy has nearly 100% specificity and sensitivity in patients with ATTRwt-CA. However, obtaining such a biopsy requires technical expertise and can cause severe complications associated with the procedure, such as cardiac tamponade and arrhythmias, albeit rarely (15). Sampling of alternative tissues has minimized the need for endomyocardial biopsies. Tissue samples can be obtained from the primarily affected organ (e.g., the heart) or more easily accessible tissues or organs, with the choice of biopsy site varying among hospitals (16). Extracardiac biopsies are more frequently performed to determine amyloid type than endomyocardial biopsies, even in specialist amyloidosis centers (14). Extracardiac biopsies, which are blindly obtained from the subcutaneous abdominal fat or the gastrointestinal tract with no imaging data suggesting the presence of ATTR deposition, are sometimes performed in patients with ATTRwt-CA. The rate of ATTR deposition is not particularly high (17, 18). Biopsy techniques that yield sufficient sample sizes of tissue with high ATTR deposition increase the ATTR detection rates; however, biopsy-induced complications, particularly organ damage and hemorrhagic complications, must be avoided.

The percutaneous skeletal muscle biopsy technique is an established procedure used to evaluate patients with diseases involving muscle tissues (19, 20). In two patients with cardiac sarcoidosis, an 18-fluorine-labeled 2-deoxy-2-fluoro-D-glucose positron emission tomography/CT imaging-based biopsy of the gluteal muscles with a focal radiotracer uptake revealed a non-caseating epithelioid cell granuloma, which is a characteristic histopathological finding in systemic sarcoi-

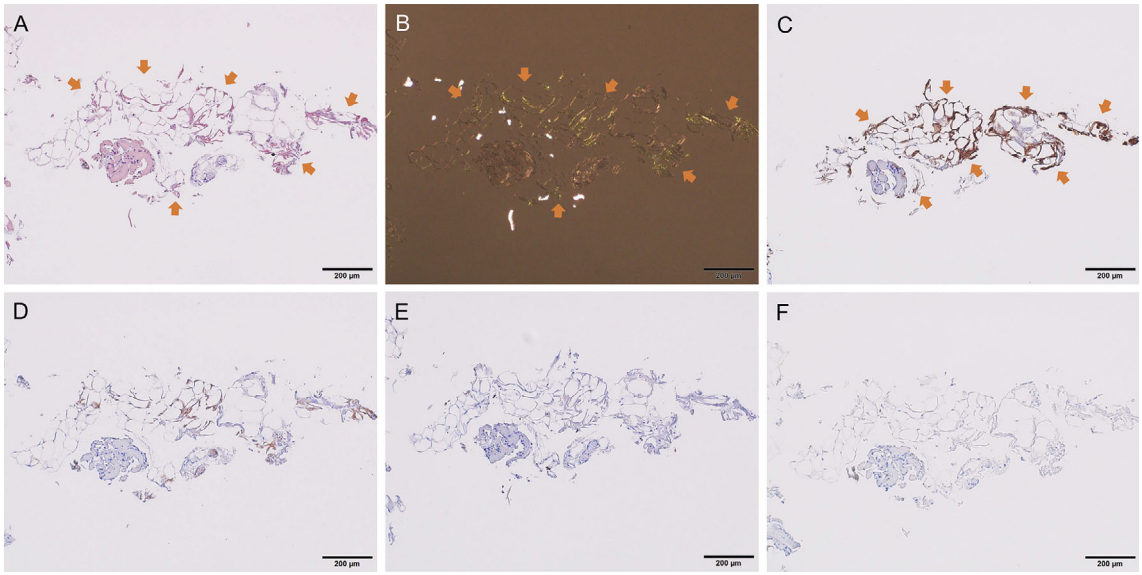

Figure 5. **Histopathological staining of tissues obtained via a computed tomography-guided core needle biopsy of the left gluteus medius muscle (Case 1). Congo red staining performed at Kumamoto University showed amyloid deposits (arrows) appearing as red-orange staining under a light microscope (A) and apple-green birefringence when visualized using a cross-polarized light microscope (B). Immunohistochemical staining after formic acid treatment for kappa light chain, lambda light chain, and transthyretin antibodies was performed for antigen retrieval at Kumamoto University using a panel of type-specific antibodies against the most common amyloidogenic proteins: anti-transthyretin 115-124 (polyclonal rabbit anti-human prealbumin, custom) (C), anti-kappa light chain 116-133 (polyclonal rabbit anti-human kappa light chains, custom) (D), anti-lambda light chain 118-134 (polyclonal rabbit anti-human lambda light chains, custom) (E), and anti-amyloid A (monoclonal mouse anti-human amyloid A, DAKO, Carpinteria, USA) (F). Only anti-transthyretin 115-124 stained the amyloid deposits (arrows). Scale bars in all panels indicate 200 μm.**

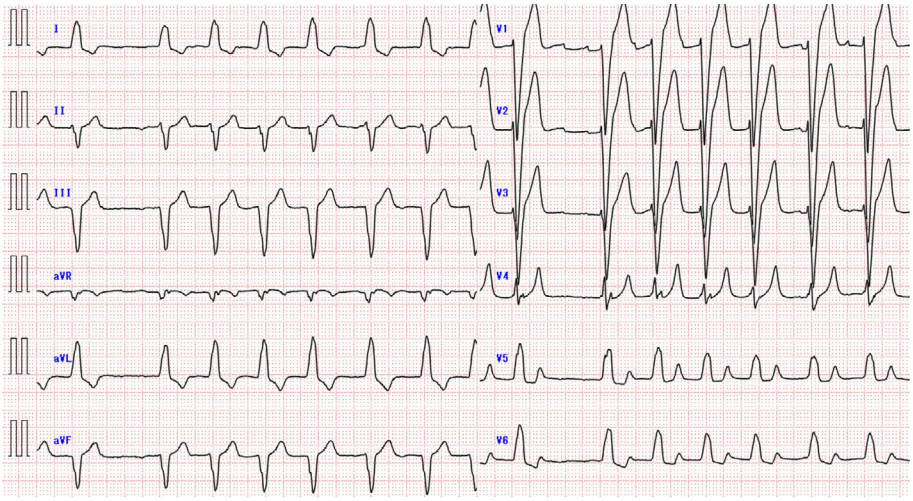

Figure 6. **Electrocardiogram findings recorded on admission (Case 2). Electrocardiography showed atrial tachycardia with P waves at a rate of 221/min (cycle length, 271 ms) and irregular ventricular rate, together with a complete left bundle branch block.**

dosis (21). Few studies have investigated the usefulness of a skeletal muscle biopsy for confirming ATTR deposition in patients with ATTRwt-CA (22). We previously reported that the extracardiac ^{99m}Tc-PYP uptake detected in patients with ATTRwt-CA indicated amyloid deposition (2-4). A ^{99m}Tc-PYP imaging-based CT-guided core needle biopsy of the internal oblique muscle with a tracer uptake in patients with ATTRwt-CA has a high ATTR detection rate (88.9%), although tracer accumulation-negative patients have not been investigated (5). In addition, no significant complications,

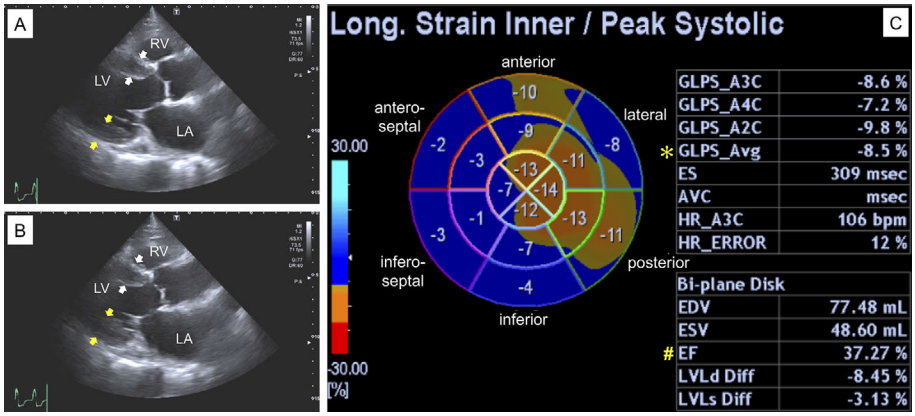

Figure 7. **Echocardiogram findings recorded on admission (Case 2). A normal-sized left ventricle with an end-diastolic dimension of 48.1 mm and an increase in the interventricular septum thickness (white arrows) and left ventricular (LV) posterior wall thickness (yellow arrows) of 13.7 and 12.3 mm, respectively, and a dilated left atrium with a volume of 62.6 mL/m^2 are shown (A, end-diastole; B, end-systole). The bull's-eye map (C), as shown in Fig. 2, showed a reduced LV ejection fraction (EF) of 37.3% (marked with a hash mark) and an LV global longitudinal peak systolic strain (GLS) value of -8.5% (marked with an asterisk) with an LVEF/|GLS| of 4.4, indicating apical sparing (cutoff, >4.1) (C). LA: left atrium, LV: left ventricle, RV: right ventricle**

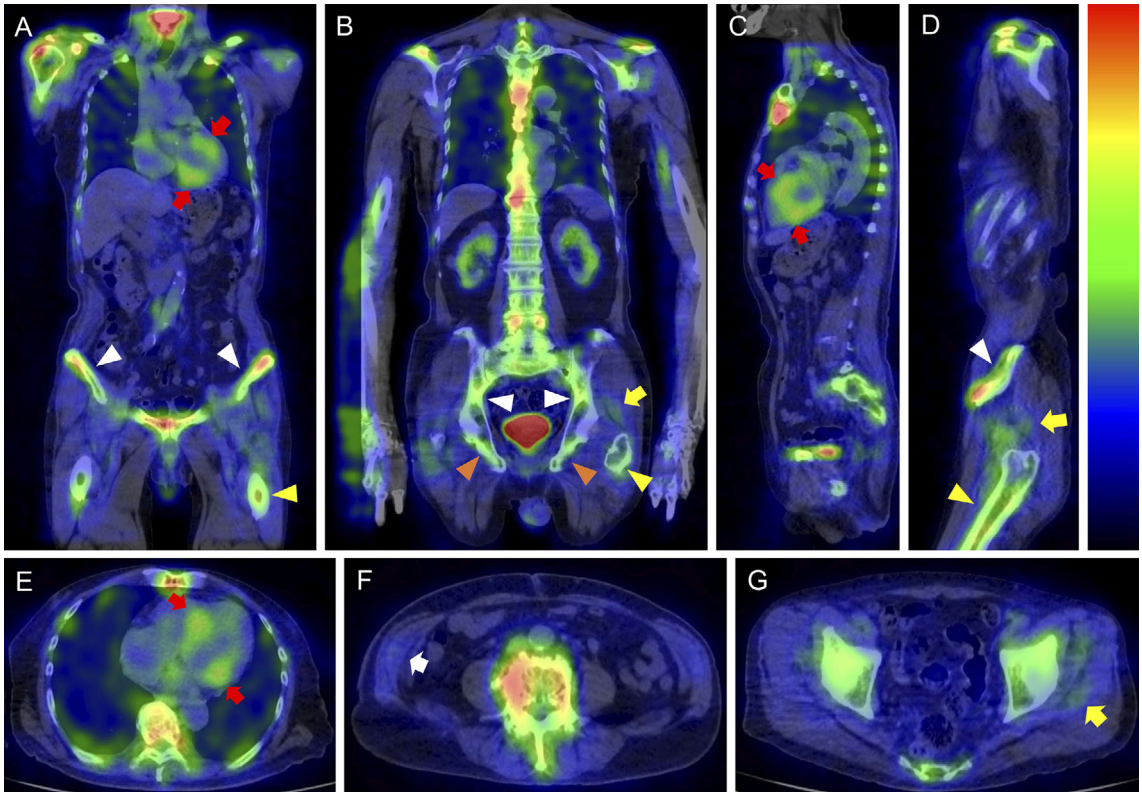

Figure 8. **Chest- and abdomen-centered single-photon emission computed tomography (SPECT)/computed tomography (CT) fusion images of technetium-99m-labeled pyrophosphate (^{99m}Tc-PYP) scintigraphy obtained 2 h after injecting the radiotracer (Case 2). (A, B) The coronal plane, (C, D) sagittal plane, and horizontal plane of (E) the heart and (F, G) abdomen/pelvis. For SPECT/CT fusion images, the method of displaying SPECT images in linear color scale and the definition of positive ^{99m}Tc-PYP accumulation in the relevant muscles are as indicated in Fig. 3. The accumulation of ^{99m}Tc-PYP in the myocardium (red arrows), abdominal oblique (white arrow), and gluteus muscles (yellow arrows) is shown. However, no tracer uptake in subcutaneous abdominal fat was detected. White, orange, and yellow arrowheads indicate the ilium, ischium, and left femur, respectively. For comparison, a representative case of wild-type transthyretin cardiac amyloidosis with almost no tracer uptake in the skeletal trunk muscles is shown (Supplementary material).**

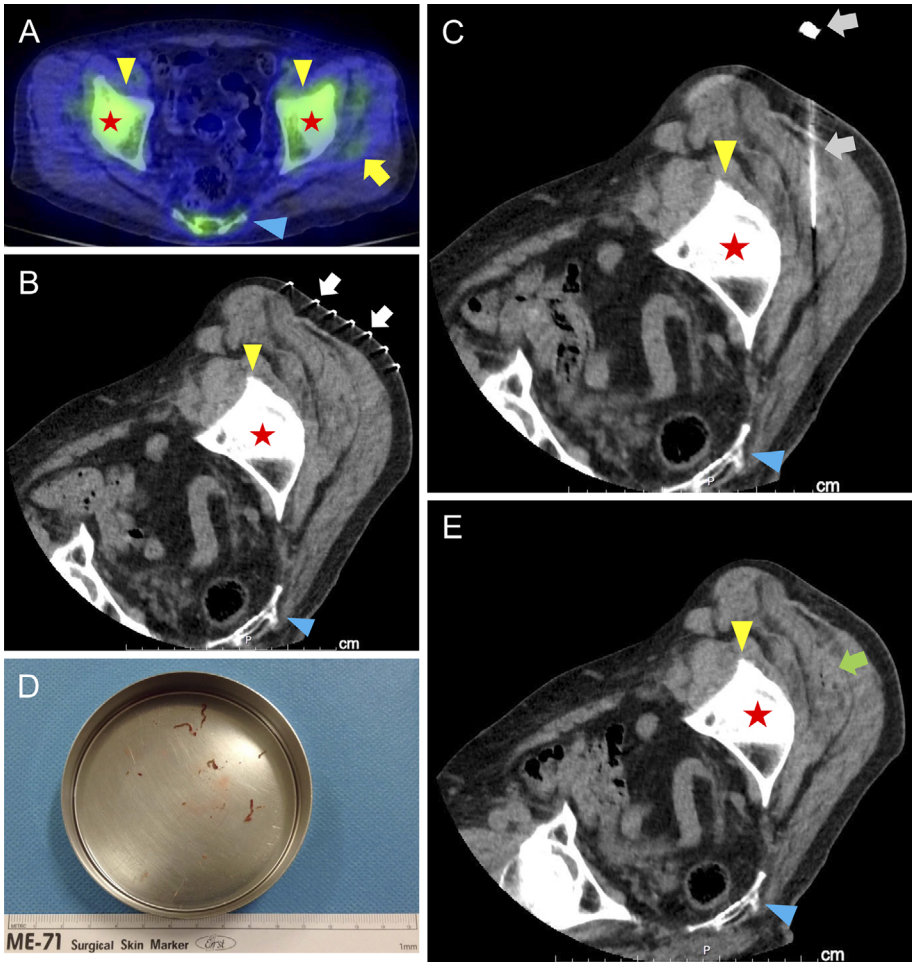

Figure 9. **A technetium-99m-labeled pyrophosphate (^{99m}Tc-PYP) imaging-based computed tomography (CT)-guided core needle biopsy of the left gluteus medius muscle (Case 2). The target of the biopsy is the site with the highest ^{99m}Tc-PYP uptake in the gluteus medius muscle (yellow arrow) (A). The patient was positioned in the supine oblique position on the CT scanner table, and the first CT images were obtained after applying the Guidelines® CT biopsy grid (Beekley Medical, Bristol, USA) to the skin of the biopsy site (white arrows) (B). The introducer stylet and cannula of the 18-gauge Fine Core® (Dr. Japan, Tokyo, Japan) spring-loaded semi-automatic biopsy needle, with a length of 10 cm, were advanced into the left gluteus medius muscle through a small pre-incision of the skin (gray arrows) (C), and a muscle specimen was obtained (D). The final CT image obtained after retracting the biopsy needle and introducer cannula showed some air (light green arrow) but no hematoma in the left gluteus medius (E). Yellow arrowheads, blue arrowheads, and stars indicate the acetabulum, sacrum, and femoral head, respectively.**

such as intramuscular hematoma, have been reported despite >70% of patients receiving anticoagulants or antiplatelet agents. These results make this biopsy useful as an extracardiac screening biopsy in ATTRwt-CA (17, 18).

In the present study, we performed a CT-guided core needle biopsy of the gluteus medius muscle instead of the internal oblique muscle in two patients with suspected ATTRwt-CA. Similar to the internal oblique muscles, the gluteal muscles are located close to the body surface, and no organs, including large blood vessels, are in close proximity, making serious complications associated with accidental puncture unlikely (23). In both cases, some ^{99m}Tc-PYP uptake was detected in the internal oblique muscle, so a biopsy of the muscle may have detected ATTR. However, tissue samples obtained from the gluteus medius muscle are expected to be more reliable in confirming ATTR deposition than those obtained from the internal oblique muscle.

The results obtained using a ^{99m}Tc-PYP imaging-based CT-guided core needle biopsy of the skeletal trunk muscles should be interpreted with caution. First, the mechanism underlying the myocardial uptake of ^{99m}Tc-PYP in ATTRwt-CA is not fully understood. ^{99m}Tc-PYP, a bone-seeking tracer, shows a physiological and pathological uptake in various tissues and organs in addition to bones (24, 25). Therefore, ^{99m}Tc-PYP accumulation does not always reflect amyloid deposition. Second, misregistration or blurring of ^{99m}Tc-PYP SPECT/CT fusion images may occur mainly due to patient movement and breathing in addition to the use of separate

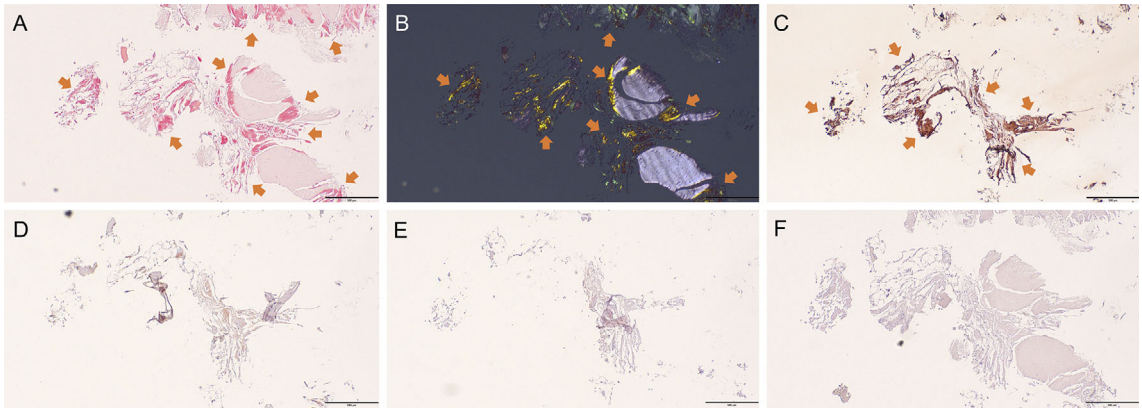

Figure 10. Histopathological staining of tissues obtained via a computed tomography-guided core needle biopsy of the left gluteus medius muscle (Case 2). Congo red staining performed at Kumamoto University showed amyloid deposition appearing as red-orange staining under a light microscope (A) and apple-green birefringence when visualized under a cross-polarized light microscope (B). Immunohistochemical staining was performed at Kumamoto University using a panel of type-specific antibodies against the most common amyloidogenic proteins, as shown in Fig. 5, which is positive for the antibody raised against the anti-transthyretin (C) and negative for antibodies raised against other amyloid proteins, anti-kappa light chain (D), anti-lambda light chain (E), and anti-amyloid A (F). Scale bars in all panels indicate 200 μm.

SPECT and CT scanners (1, 3, 5), as shown in Figs. 3 and 8. Thus, using the fusion image as guidance may result in sampling error. Third, an increased ^{99m}Tc-PYP uptake by organs or tissues, such as the bone, kidneys, and bladder, influences the visual assessment of the tracer uptake in the neighboring organs or tissues and decreases the accuracy of regional amyloid deposition detection. Nevertheless, a ^{99m}Tc-PYP imaging-based CT-guided core needle biopsy of the skeletal trunk muscles with a tracer uptake can be used to confirm ATTR deposition with relatively high sensitivity.

When ATTR deposition needs to be confirmed in patients with suspected ATTRwt-CA, we propose proceeding with biopsies in the following order: in patients with a subcutaneous abdominal fat ^{99m}Tc-PYP uptake, particularly those showing mottled or diffuse uptake patterns, as in Case 1, a subcutaneous abdominal fat fine-needle aspiration biopsy, which is a safe and quick bedside procedure, may be selected as the first screening biopsy method (3); for patients with no ^{99m}Tc-PYP uptake in the subcutaneous abdominal fat, as shown in Case 2, or negative subcutaneous abdominal fat fine-needle aspiration biopsy results, endomyocardial or other extracardiac biopsies should be selected by the mutual decision of patients and medical staff. Regarding extracardiac biopsies, a ^{99m}Tc-PYP imaging-based CT-guided core needle biopsy of the skeletal trunk muscle with a radiotracer uptake can be selected as the preferred method because of its higher sensitivity for detecting ATTR deposits than other biopsy methods (17, 18) and low incidence of complications (5). Future studies should develop an algorithm for choosing a biopsy approach to histologically confirm ATTR deposition in patients with suspected ATTRwt-CA.

In conclusion, the present study expands the possibility of using a ^{99m}Tc-PYP imaging-based CT-guided core needle biopsy of the skeletal trunk muscles, including the gluteal muscles, showing the uptake of tracer to confirm ATTR deposition.

Informed consent was obtained from the patients and their families for the publication of this case report. This case report was written while maintaining respect for patient confidentiality and privacy. The patients and their families had the opportunity to read this report and had no objections to the final form.

The authors state that they have no Conflict of Interest (COI).

Acknowledgement

We express our sincere thanks to Ms. Miki Kaneno and Ms. Yumie Hiraoka for their assistance with the study and to the clinical staff at Yawatahama City General Hospital.

References

1. Takahashi K, Hiratsuka Y, Sasaki D, et al. ^{99m}Tc-pyrophosphate scintigraphy can image tracer uptake in skeletal trunk muscles of transthyretin cardiac amyloidosis. Clin Nucl Med **48**: 18-24, 2023.
2. Takahashi K, Sasaki D, Sakaue T, et al. Extracardiac accumulation of technetium-99m-pyrophosphate in transthyretin cardiac amyloidosis. JACC Case Rep **3**: 1069-1074, 2021.
3. Takahashi K, Sasaki D, Yamashita M, et al. Amyloid deposit corresponds to technetium-99m-pyrophosphate accumulation in abdominal fat of patients with transthyretin cardiac amyloidosis. J Nucl Cardiol **29**: 3126-3136, 2022.
4. Takahashi K, Morioka H, Sasaki D, et al. Two autopsy cases of wild-type transthyretin cardiac amyloidosis who died 10 days after technetium-99m-pyrophosphate scintigraphy. J Nucl Cardiol **30**: 2215-2221, 2023.
5. Takahashi K, Hiratsuka Y, Iwamura T, et al. Technetium-99m-pyrophosphate imaging-based computed tomography-guided core-

needle biopsy of internal oblique muscle in wild-type transthyretin cardiac amyloidosis. Amyloid **31**: 12-21, 2024.
6. Ungericht M, Wanschitz J, Kroiss AS, et al. Amyloid myopathy: expanding the clinical spectrum of transthyretin amyloidosis - case report and literature review. J Nucl Cardiol **30**: 1420-1426, 2023.
7. Dorbala S, Ando Y, Bokhari S, et al. ASNC/AHA/ASE/EANM/HFSA/ISA/SCMR/SNMMI expert consensus recommendations for multimodality imaging in cardiac amyloidosis: part 1 of 2-evidence base and standardized methods of imaging. Circ Cardiovasc Imaging **14**: e000029, 2021.
8. Buxbaum JN, Dispenzieri A, Eisenberg DS, et al. Amyloid nomenclature 2022: update, novel proteins, and recommendations by the International Society of Amyloidosis (ISA) Nomenclature Committee. Amyloid **29**: 213-219, 2022.
9. Pitkänen P, Westermark P, Cornwell GG 3rd. Senile systemic amyloidosis. Am J Pathol **117**: 391-399, 1984.
10. Ueda M, Horibata Y, Shono M, et al. Clinicopathological features of senile systemic amyloidosis: an ante- and post-mortem study. Mod Pathol **24**: 1533-1544, 2011.
11. Sueyoshi T, Ueda M, Jono H, et al. Wild-type transthyretin-derived amyloidosis in various ligaments and tendons. Hum Pathol **42**: 1259-1264, 2011.
12. Koike H, Katsuno M. Ultrastructure in transthyretin amyloidosis: from pathophysiology to therapeutic insights. Biomedicines **7**: 11, 2019.
13. Benson MD, Berk JL, Dispenzieri A, et al. Tissue biopsy for the diagnosis of amyloidosis: experience from some centres. Amyloid **29**: 8-13, 2022.
14. Rauf MU, Hawkins PN, Cappelli F, et al. Tc-99m labelled bone scintigraphy in suspected cardiac amyloidosis. Eur Heart J **44**: 2187-2198, 2023.
15. Porcari A, Baggio C, Fabris E, et al. Endomyocardial biopsy in the clinical context: current indications and challenging scenarios. Heart Fail Rev **28**: 123-135, 2023.
16. Quarta CC, Gonzalez-Lopez E, Gilbertson JA, et al. Diagnostic sensitivity of abdominal fat aspiration in cardiac amyloidosis. Eur Heart J **38**: 1905-1908, 2017.
17. Nishi M, Takashio S, Morioka M, et al. Extracardiac biopsy sensitivity in transthyretin amyloidosis cardiomyopathy patients with positive ^{99m}Tc-labeled pyrophosphate scintigraphy findings. Circ J **86**: 1113-1120, 2022.
18. Kitaoka H, Izumi C, Izumiya Y, et al.; the Japan Circulation Society Joint Working Group. JCS 2020 guideline on diagnosis and treatment of cardiac amyloidosis. Circ J **84**: 1610-1671, 2020.
19. Tarnopolsky MA, Pearce E, Smith K, Lach B. Suction-modified Bergström muscle biopsy technique: experience with 13,500 procedures. Muscle Nerve **43**: 717-725, 2011.
20. Ekblom B. The muscle biopsy technique. Historical and methodological considerations. Scand J Med Sci Sports **27**: 458-461, 2017.
21. Takahashi T, Okayama H, Hiasa G, Kazatani Y. Two cases of cardiac sarcoidosis diagnosed based on biopsy results of the gluteus muscle with focal uptake of ^{18}F-fluorodeoxyglucose. Eur Heart J **37**: 1168, 2016.
22. Hutt DF, Fontana M, Burniston M, et al. Prognostic utility of the Perugini grading of ^{99m}Tc-DPD scintigraphy in transthyretin (ATTR) amyloidosis and its relationship with skeletal muscle and soft tissue amyloid. Eur Heart J Cardiovasc Imaging **18**: 1344-1350, 2017.
23. Solomon LB, Hofstaetter JG, Bolt MJ, Howie DW. An extended posterior approach to the hip and pelvis for complex acetabular reconstruction that preserves the gluteal muscles and their neurovascular supply. Bone Joint J **96-B**: 48-53, 2014.
24. Gnanasegaran G, Cook G, Adamson K, Fogelman I. Patterns, variants, artifacts, and pitfalls in conventional radionuclide bone imaging and SPECT/CT. Semin Nucl Med **39**: 380-395, 2009.
25. Khor YM, Dorbala S. Extra-cardiac uptake on technetium-99m pyrophosphate (Tc-99m PYP) scan: not just a matter of the heart. J Nucl Cardiol **30**: 2540-2543, 2023.